

Effect of flatness of heterointerfaces on device performance of InP-based HEMTs

Issei Watanabe^{1,*}, Keisuke Shinohara^{1,†}, Takahiro Kitada², Satoshi Shimomura², Akira Endoh³, Yoshimi Yamashita³, Takashi Mimura³, Satoshi Hiyamizu², and Toshiaki Matsui¹

¹National Institute of Info. & Com. Tech., 4-2-1, Nukui-kitamachi, Koganei, Tokyo 184-8795, Japan

²Osaka University, 1-3, Machikaneyama, Toyonaka, Osaka 560-8531, Japan

³Fujitsu Laboratories Limited, 10-1, Morinosato-wakamiya, Atsugi, Kanagawa 243-0197, Japan

1. Introduction

InP-based InGaAs/InAlAs high electron mobility transistors (HEMTs) demonstrate very high cutoff frequencies (f_T) up to 562 GHz at room temperature [1, 2]. Such a high f_T was achieved by reducing the gate length (L_g) of 25 nm and the gate-to-channel distance of 4 nm, which led to the suppression of short channel effects and the enhancement of overshoot in electron velocity. For achieving further device performance, cryogenic operations can be expected to enhance not only transconductance (g_m) but also f_T due to suppression of phonon scattering. Recently we have proposed an application of (411)A super-flat interfaces (effectively atomically flat heterointerfaces over a wafer-size area) to cryogenically cooled HEMTs because interface roughness scattering is a dominant factor to limit electron mobility at cryogenic temperatures. In fact, we reported an extremely high g_m of 2.25 S/mm at 16 K for an In_{0.75}Ga_{0.25}As/In_{0.52}Al_{0.48}As HEMT with $L_g = 195$ nm fabricated on the (411)A-oriented InP substrate using molecular beam epitaxy (MBE) [3]. In this study, we investigated the dc and radio frequency (RF) characteristics of the 195-nm-gate In_{0.75}Ga_{0.25}As/In_{0.52}Al_{0.48}As HEMTs fabricated on the (411)A- and conventional (100)-oriented InP substrates at 300 K and 16 K.

2. Device performance

The In_{0.75}Ga_{0.25}As/In_{0.52}Al_{0.48}As HEMT structure consists of an 8-nm-thick pseudomorphic In_{0.75}Ga_{0.25}As channel separated from a Si-planar doped sheet ($N_D = 1 \times 10^{13}$ cm⁻²) by a 3-nm-thick undoped In_{0.52}Al_{0.48}As spacer layer. For achieving high-speed performance at both room and cryogenic temperatures, we designed a gate-to-channel distance of 13 nm. We measured the on-wafer dc and RF characteristics of 300 K and 16 K using a vector network analyzer (HP8510C) and a specially designed probing system with a vacuum chamber, a helium-gas closed cryostat, and on-wafer probes.

A. Room temperature (300 K)

Fig. 1 shows the current-voltage (I - V) characteristics at 300 K for the (411)A and (100) HEMTs with $L_g = 195$ nm and the drain-source currents (I_{ds}) were well pinched off. For the (411)A HEMT, the extrinsic g_m was 1.78 S/mm under a

drain-source voltage (V_{ds}) of 0.8 V and a gate-source voltage (V_{gs}) of -0.25 V, which was 10% higher than that of the corresponding (100) HEMT (1.62 S/mm at $V_{ds} = 0.8$ V and $V_{gs} = -0.15$ V). We then measured the S -parameters in the frequency range of 0.25 to 50.25 GHz using a short-open-load-through (SOLT) method to determine the value of f_T by extrapolating the current gain ($|h_{21}|^2$) using a least-squares fitting with a -20 dB/decade slope after subtracting the parasitic capacitances due to the probing pads. The f_T of the (411)A HEMT was 245 GHz when biased under $V_{ds} = 0.8$ V and $V_{gs} = -0.25$ V, which was almost the same as that of the (100) HEMT (233 GHz at $V_{ds} = 0.8$ V and $V_{gs} = -0.15$ V). Furthermore, these f_T were almost the same as those previously reported for (100) HEMTs with similar L_g [2].

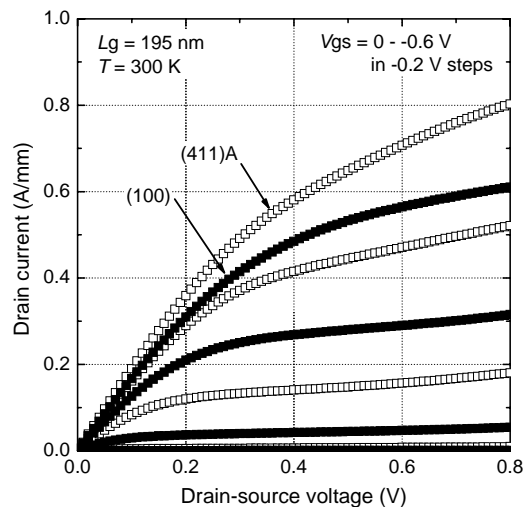


Fig. 1 I - V characteristics at 300 K for the (411)A and (100) In_{0.75}Ga_{0.25}As/In_{0.52}Al_{0.48}As HEMTs with $L_g = 195$ nm.

B. Cryogenic temperature (16 K)

The I_{ds} was also pinched off at 16 K for each sample as shown in Fig. 2. As temperature decreased, the extrinsic g_m increased and reached 2.25 S/mm at 16 K for the (411)A HEMT with $L_g = 195$ nm, which was 26% higher than the 300 K value. The g_m as high as 2.25 S/mm, to our knowledge, is one of the highest values for HEMTs ever reported. The f_T was 310 GHz at 16 K for the (411)A HEMT with $L_g = 195$ nm, which was 27% higher than the room temperature value. On the other hand, the g_m and f_T were 2.02 S/mm and 268 GHz at 16 K for the (100) HEMT with $L_g = 195$ nm, which were respectively 25% and 15% higher than

*Corresponding author. E-mail: issei@nict.go.jp.

Phone: +81-42-327-7944. Fax: +81-42-327-6669.

†Present address: Rockwell Scientific Company,

1049 Camino Dos Rios, Thousand Oaks, CA91360, USA

the 300 K values. These results indicate that the enhancement of g_m and f_T at low temperatures was possibly due to the increased electron mobility and/or velocity because of the suppression of phonon scattering.

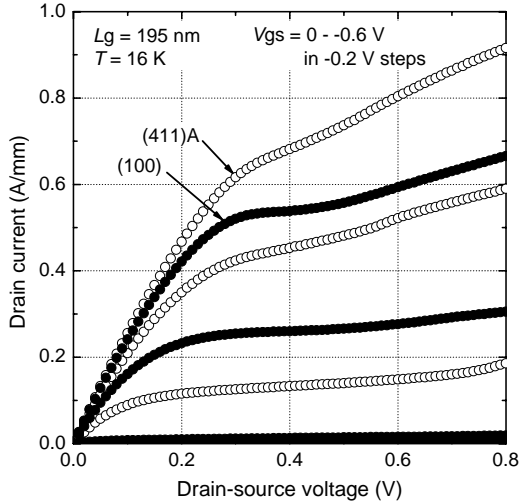


Fig. 2 I - V characteristics at 16 K for the (411)A and (100) $\text{In}_{0.75}\text{Ga}_{0.25}\text{As}/\text{In}_{0.52}\text{Al}_{0.48}\text{As}$ HEMTs with $L_g = 195$ nm.

3. Delay time analysis

In order to understand the cause of the enhanced g_m and f_T at 16 K, we carried out delay time analysis using a method described by Enoki et al [4]. The delay time (τ) can be expressed as

$$\tau = \frac{1}{2\pi f_T} = \tau_i + \tau_p = (\tau_{\text{transit}} + \tau_{cc}) + C_{gd} \cdot (R_s + R_d). \quad (1)$$

The intrinsic delay time (τ_i) is the sum of the transit time in the region under the gate (τ_{transit}) and the channel charging time (τ_{cc}). The parasitic delay time (τ_p) is given as $C_{gd} \cdot (R_s + R_d)$, where C_{gd} is the gate-drain capacitance, R_s is the source resistance, and R_d is the drain resistance. We summarized the results of the delay time analysis at 300 K and 16 K for the (411)A and (100) HEMTs with $L_g = 195$ nm in Table I. As the result of the delay time analysis, we found that the f_T value was mainly dominated by the τ_{transit} at both 300 K and 16 K, which means that the enhanced g_m and f_T were due to the increased velocity under the gate. The f_T of 245 GHz was obtained at 300 K, which was almost the same as that of the corresponding (100) HEMT (233 GHz), indicating that the average electron velocity (v_{ave}) of the (411)A HEMT (3.8×10^7 cm/s), determined by the delay time analysis, was almost the same as the v_{ave} of the (100) HEMT (3.6×10^7 cm/s). On the other hand, the f_T as high as 310 GHz at 16 K was attributed to the v_{ave} of 4.9×10^7 cm/s, which was about 10% higher than that of the (100) HEMT (4.5×10^7 cm/s at 16 K). The high v_{ave} of 4.9×10^7 cm/s was due to suppression of phonon scattering and interface roughness scattering because of the (411)A super-flat interfaces. These results suggest that the (411)A In-GaAs/InAlAs HEMTs may be applicable to not only future

high-speed and high-frequency wireless communications but also cryogenically cooled amplifiers with high-gain and low-noise performances in the field of radio astronomy.

Table I Intrinsic delay time (τ_i) and parasitic delay time (τ_p) at 300 K and 16 K for the (411)A and (100) $\text{In}_{0.75}\text{Ga}_{0.25}\text{As}/\text{In}_{0.52}\text{Al}_{0.48}\text{As}$ HEMTs with $L_g = 195$ nm.

		intrinsic		parasitic		
		τ_{transit} (ps)	τ_i (ps)	C_{gd} (fF)	R_s+R_d (Ωmm)	τ_p (ps)
(411)A	300 K	0.48	0.10	28	0.27	0.08
	16 K	0.39	0.07	28	0.18	0.05
(100)	300 K	0.55	0.06	22	0.34	0.08
	16 K	0.43	0.12	27	0.17	0.04

4. Conclusions

We obtained significantly enhanced g_m and f_T for both (411)A and (100) HEMTs at 16 K, which were caused by the increased v_{ave} mainly due to suppression of phonon scattering. Moreover, higher f_T as high as 310 GHz was attributed to the increased v_{ave} of 4.9×10^7 cm/s at 16 K for the (411)A HEMTs compared with the corresponding (100) HEMTs, which was caused by much reduced interface roughness scattering of electrons due to the (411)A super-flat interfaces.

Acknowledgements

This work was partially supported by The research and development project for expansion of radio spectrum resources of the Ministry of Internal Affairs and Communications, Japan.

References

- [1] Y. Yamashita, A. Endoh, K. Shinohara, K. Hikosaka, T. Matsui, S. Hiyamizu, and T. Mimura, IEEE Electron Device Lett., **23** (2002) 573.
- [2] K. Shinohara, Y. Yamashita, A. Endoh, I. Watanabe, K. Hikosaka, T. Matsui, T. Mimura, and S. Hiyamizu, IEEE Electron Device Lett., **25** (2004) 241.
- [3] I. Watanabe, K. Shinohara, T. Kitada, S. Shimomura, Y. Yamashita, A. Endoh, T. Mimura, T. Matsui, and S. Hiyamizu, IEEE Electron Device Lett., **26** (2005) 425.
- [4] T. Enoki, K. Arai, and Y. Ishii, IEEE Electron Device Lett., **11** (1990) 502.